Supplemental Material

© Copyright 2023 American Meteorological Society (AMS)
For permission to reuse any portion of this work, please contact permissions@ametsoc.org. Any use of material in this work that is determined to be “fair use” under Section 107 of the U.S. Copyright Act (17 USC §107) or that satisfies the conditions specified in Section 108 of the U.S. Copyright Act (17 USC §108) does not require AMS’s permission. Republication, systematic reproduction, posting in electronic form, such as on a website or in a searchable database, or other uses of this material, except as exempted by the above statement, requires written permission or a license from AMS. All AMS journals and monograph publications are registered with the Copyright Clearance Center (https://www.copyright.com). Additional details are provided in the AMS Copyright Policy statement, available on the AMS website (https://www.ametsoc.org/PUBSCopyrightPolicy).

Supplemental material for

Understanding the variation and mechanisms of tropical cyclone genesis potential over the western North Pacific during the past 20,000 years

Dubin Huan [a, d], Qing Yan [a, b, *], Ting Wei [c], Nanxuan Jiang [a, d]

[a] Nansen-Zhu International Research Centre, Institute of Atmospheric Physics, Chinese Academy of Sciences, Beijing, China

[b] Key Laboratory of Meteorological Disaster/Collaborative Innovation Center on Forecast and Evaluation of Meteorological Disasters, Nanjing University of Information Science and Technology, Nanjing, China

[c] State Key Laboratory of Severe Weather, Chinese Academy of Meteorological Sciences, Beijing, China

[d] University of Chinese Academy of Sciences, Beijing, China

Contents of this file

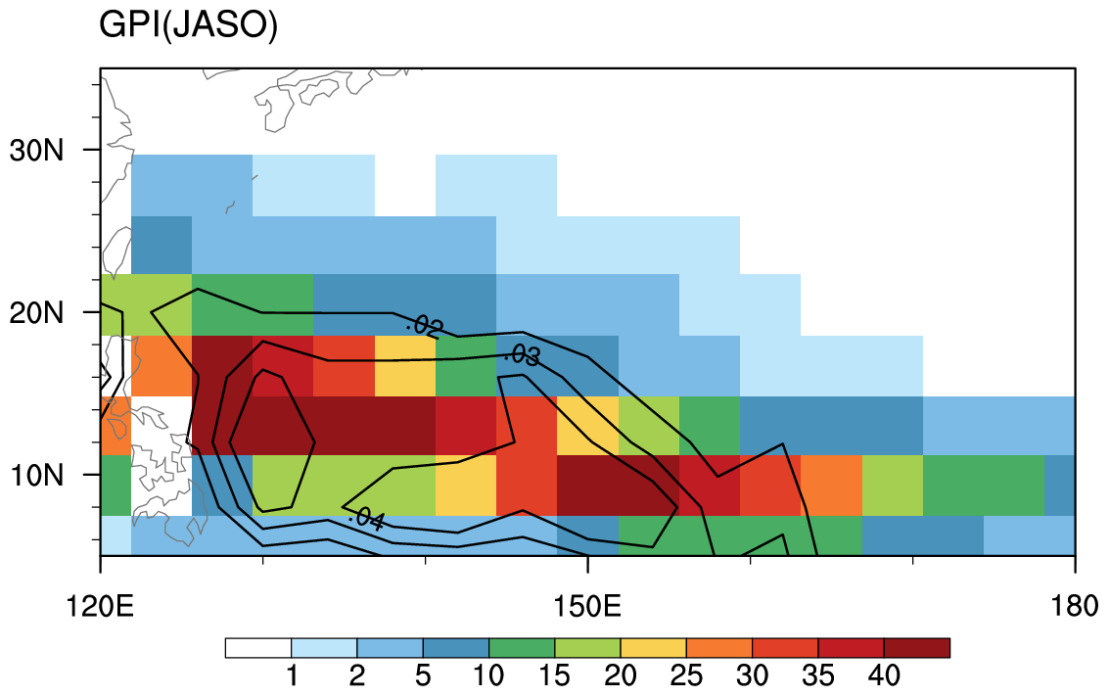

Figure S1. Observed TC genesis density (contours; units: number of events per year per 1° lat squared) and modern GPI (shading) in the storm season (JASO) based on TraCE-21ka during 1951–1990. The units of GPI are events m^{-2} $season^{-1}$ 10^{-13}.

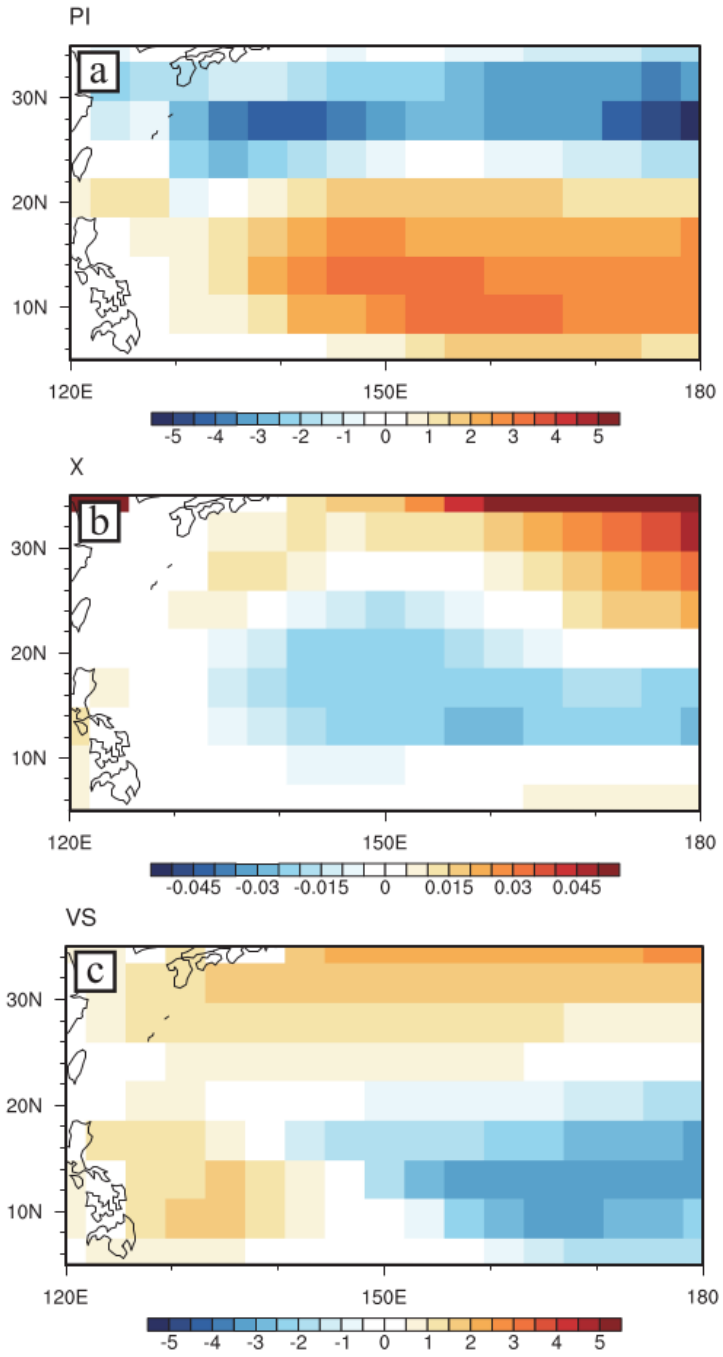

Figure S2. Differences in (a) potential intensity (units: m s^{-1}), (b) moist entropy deficit, and (c) vertical wind shear (units: m s^{-1}) between the Heinrich Stadial 1 (17–16 ka) and the last glacial maximum (19–18 ka) during summer and autumn seasons (JJASON) in the TraCE-MWF experiment.

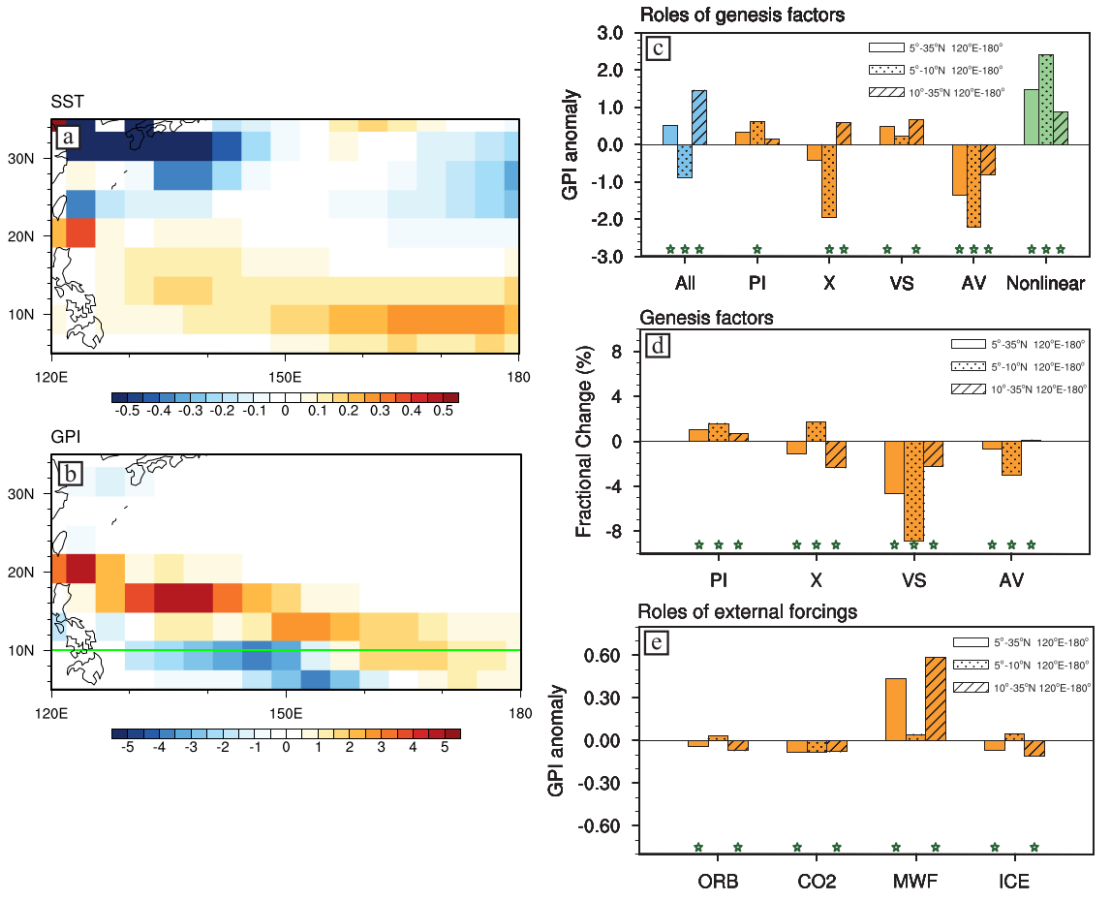

Figure S3. (a) Differences in SST (units: °C) between the Younger Dryas (YD; 12.9–11.9 ka) and the Bølling-Allerød (BA; 14–13 ka). (b) Differences in GPI between the YD and the BA. (c) Differences in GPI between the YD and the BA (blue bars) resulting from changes in potential intensity (PI), moist entropy deficit (χ), vertical wind shear (VS), absolute vorticity (AV), and nonlinear effect (see Sect. 2.c. for details). (d) Fractional changes in PI, χ, VS and AV between the YD and the BA (units: %). (e) Differences in GPI between the YD and the BA during summer and autumn seasons (JJASON) in four sensitivity experiments. Non-filled, dotted, and slant bars show the regional mean over 5°–35°N 120°E–180°, 5°–10°N 120°E–180°, and 10°–35°N 120°E–180°, respectively. Green stars represent the averaged differences are significant at 95% significance level based on the Student's *t*-test. The units of GPI are events m^{-2} $season^{-1}$ 10^{-13} in (b),(c) and 0.5 events m^{-2} $month^{-1}$ 10^{-13} in (e).

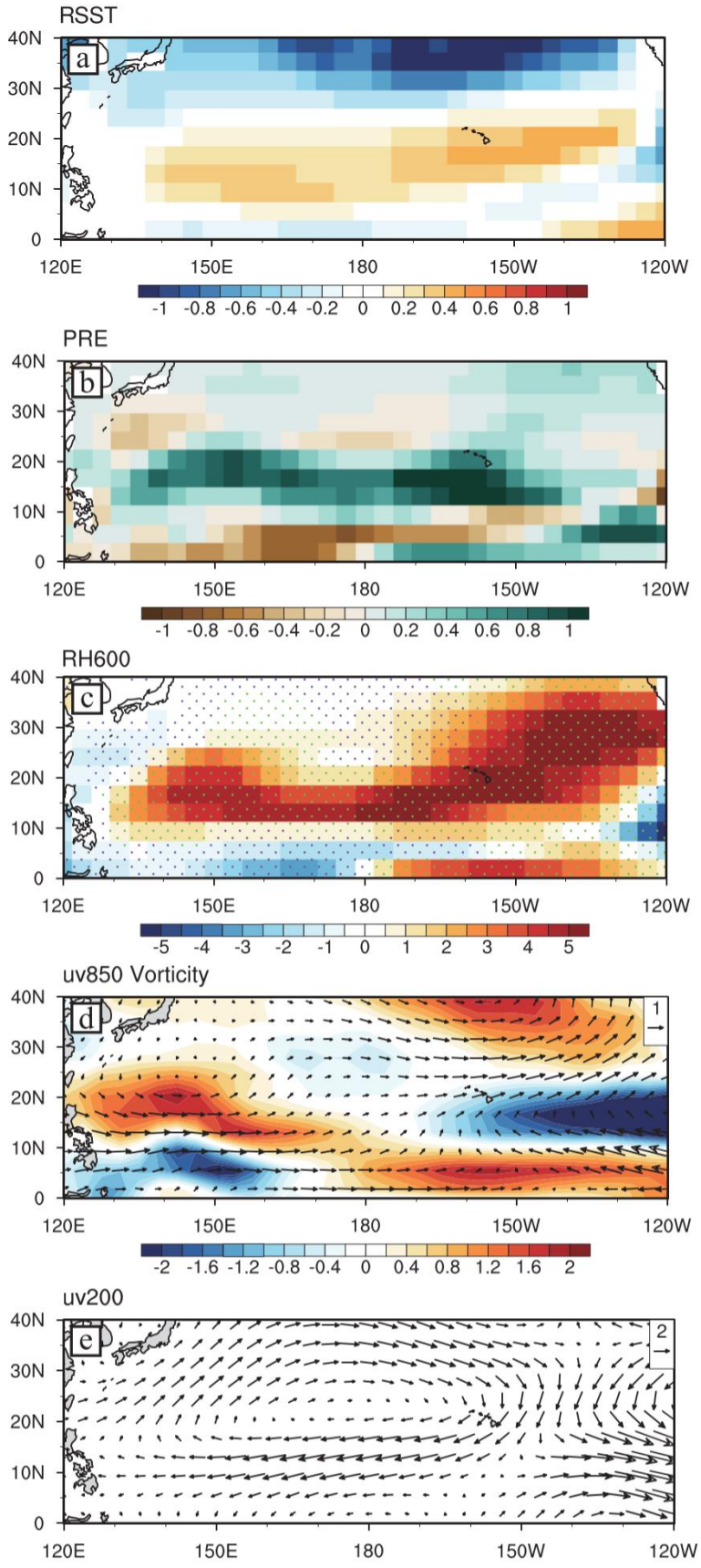

Figure S4. Differences in large-scale environmental conditions between the Younger Dryas (12.9–11.9 ka) and the Bølling-Allerød (14–13 ka) during summer and autumn

seasons (JJASON) in the TraCE-MWF experiment. (a) Relative SST (units: ℃). (b) Precipitation (shading; units: mm day^{-1}). (c) Relative humidity at 600 hPa (shading; units: %) and vertical motion (dots; green represents upward motion and purple represents downward). (d) Wind field at 850 hPa (vectors; units: m s^{-1}) and relative vorticity (shading; units: 10^{-6} s^{-1}). (e) Wind field at 200 hPa (units: m s^{-1}).

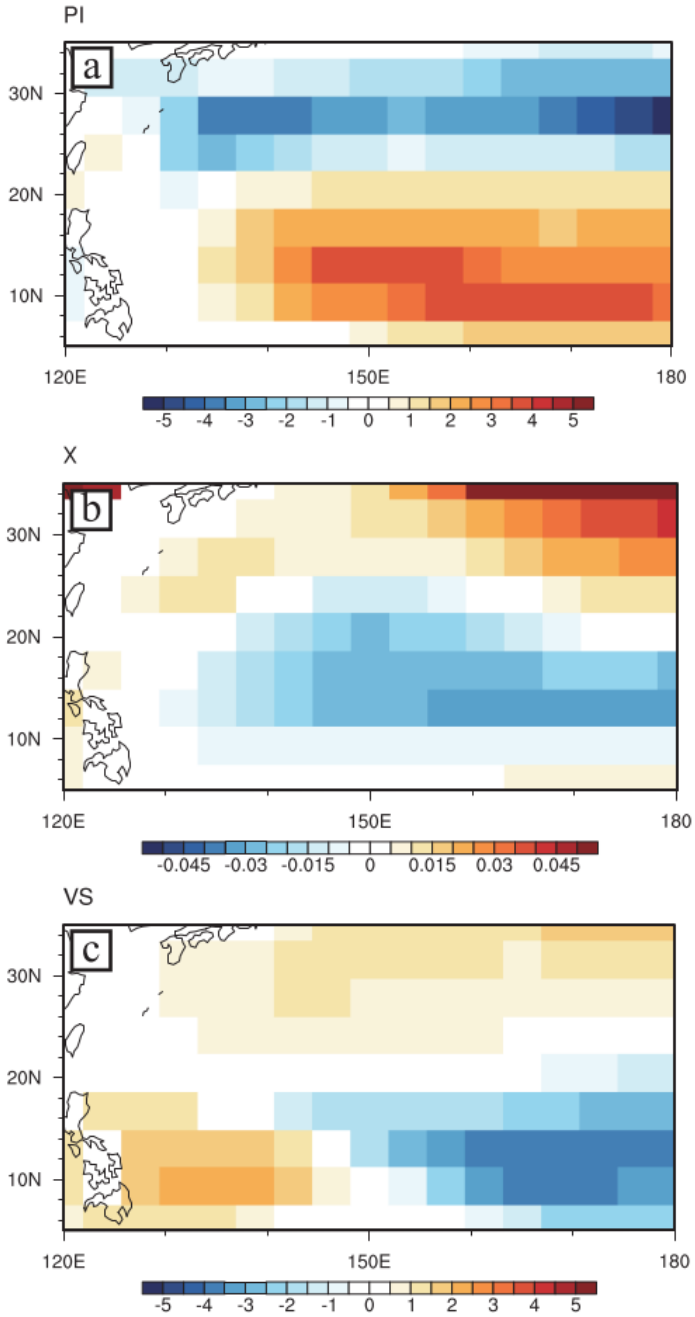

Figure S5. Differences in (a) potential intensity (units: m s^{-1}), (b) moist entropy deficit, and (c) vertical wind shear (units: m s^{-1}) between the Younger Dryas (12.9–11.9 ka) and the Bølling-Allerød (14–13 ka) during summer and autumn seasons (JJASON) in the TraCE-MWF experiment.

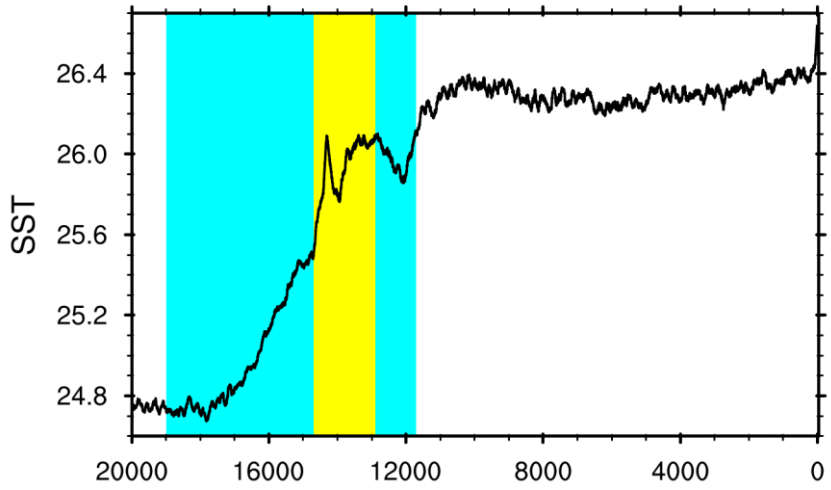

Figure S6. Evolution of sea surface temperature (units: ℃) over the western North Pacific (5°–35°N, 120°E–180°) during the past 20 ka (101-year running average). The cold events (Heinrich Stadial 1 and Younger Dryas) and the warm event (Bølling-Allerød) are marked as the cyan and yellow vertical panels, respectively.

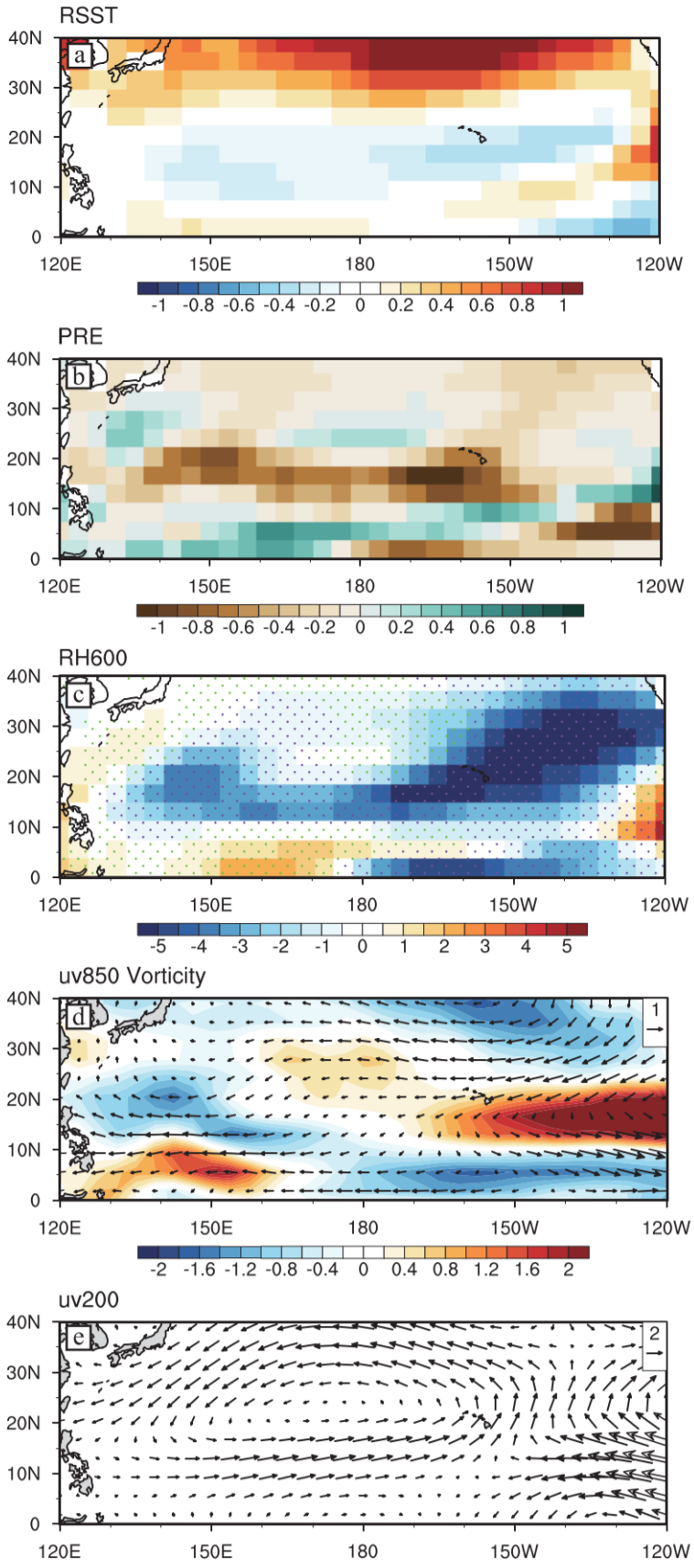

Figure S7. Differences in large-scale environmental conditions between the Bølling-Allerød (14–13 ka) and the Heinrich Stadial 1 (17–16 ka) during summer and

autumn seasons (JJASON) in the TraCE-MWF experiment. (a) Relative SST (units: ℃). (b) Precipitation (shading; units: mm day^{-1}). (c) Relative humidity at 600 hPa (shading; units: %) and vertical motion (dots; green represents upward motion and purple represents downward). (d) Wind field at 850 hPa (vectors; units: m s^{-1}) and relative vorticity (shading; units: 10^{-6} s^{-1}). (e) Wind field at 200 hPa (units: m s^{-1}).

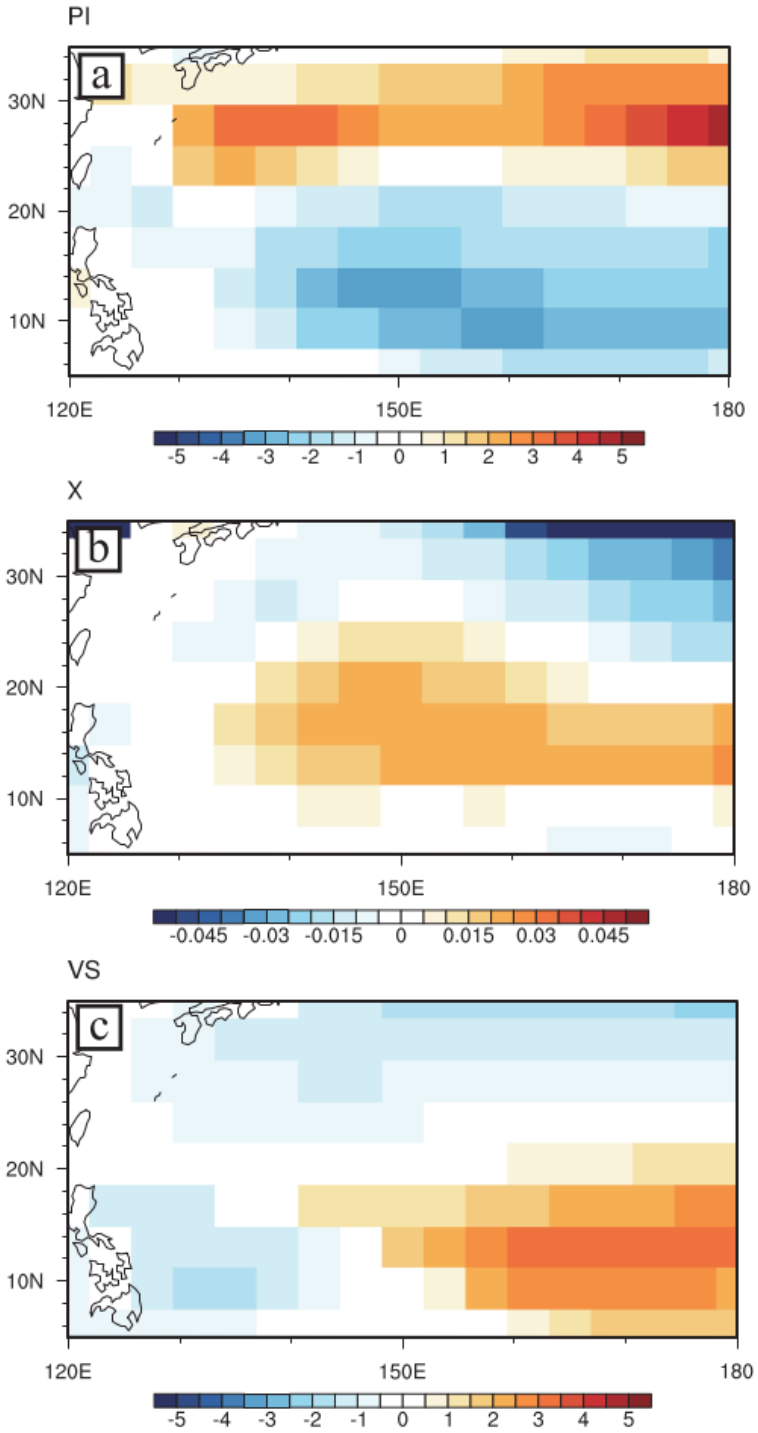

Figure S8. Differences in (a) potential intensity (units: m s^{-1}), (b) moist entropy deficit, and (c) vertical wind shear (units: m s^{-1}) between the Bølling-Allerød (14–13 ka) and the Heinrich Stadial 1 (17–16 ka) during summer and autumn seasons (JJASON) in the TraCE-MWF experiment.

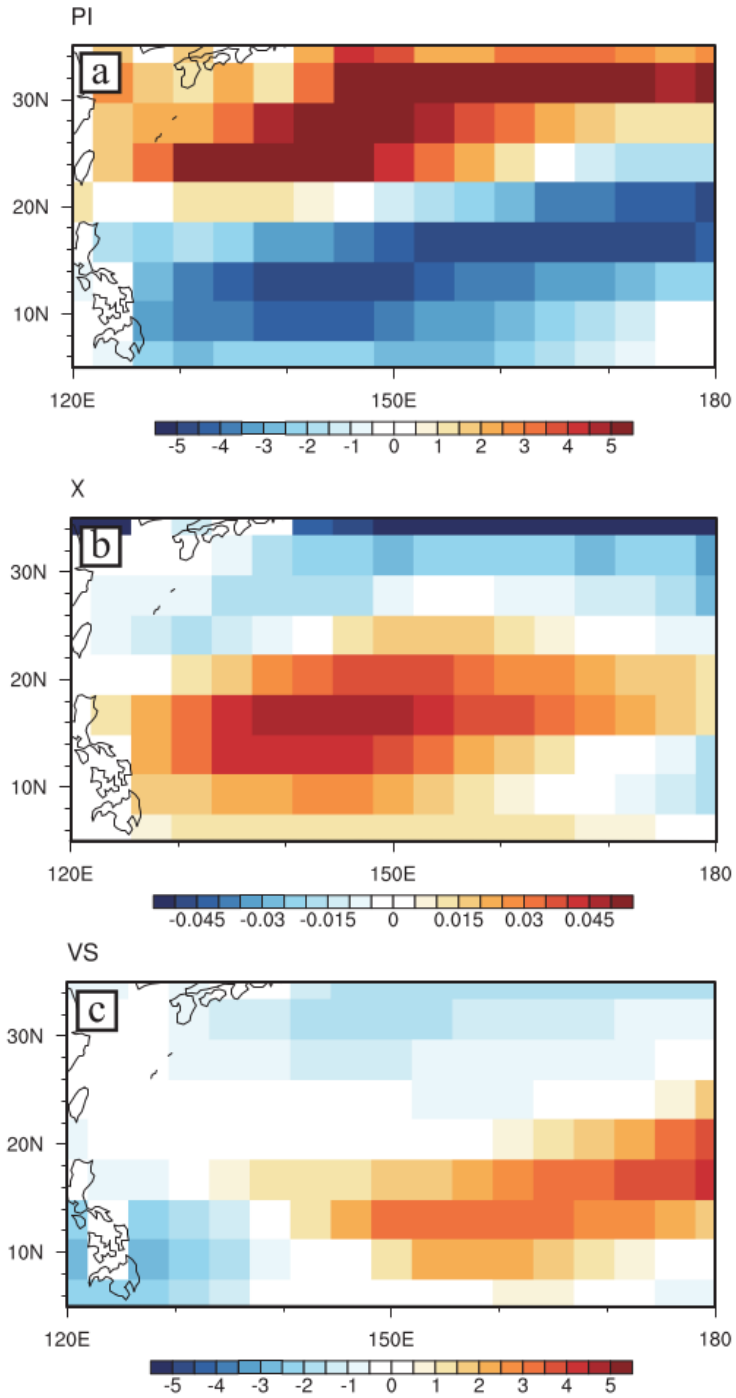

Figure S9. Differences in (a) potential intensity (units: m s^{-1}), (b) moist entropy deficit, and (c) vertical wind shear (units: m s^{-1}) between the Bølling-Allerød (14–13 ka) and the Heinrich Stadial 1 (17–16 ka) during summer and autumn seasons (JJASON) in the TraCE-ICE experiment.

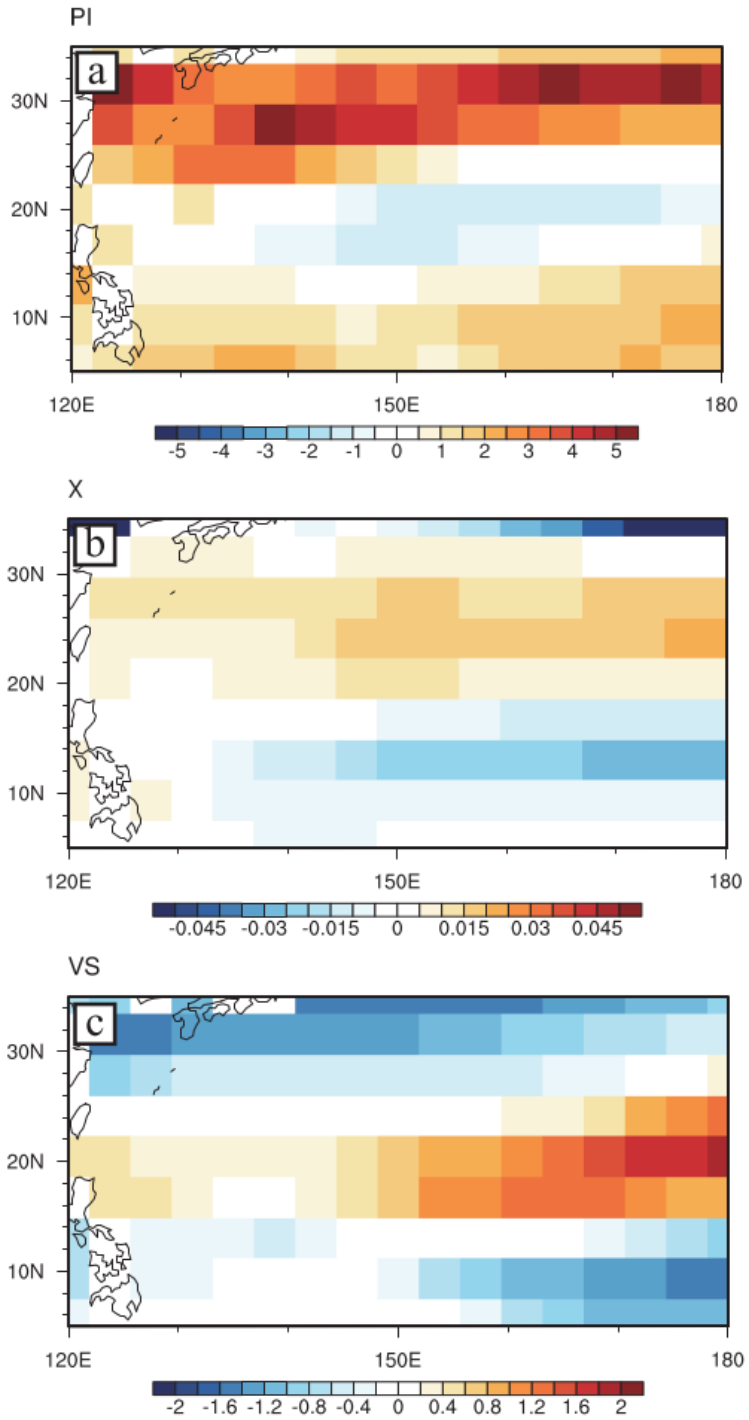

Figure S10. Differences in (a) potential intensity (units: m s^{-1}), (b) moist entropy deficit, and (c) vertical wind shear (units: m s^{-1}) between the Bølling-Allerød (14–13 ka) and the Heinrich Stadial 1 (17–16 ka) during summer and autumn seasons (JJASON) in the TraCE-CO_2 experiment.

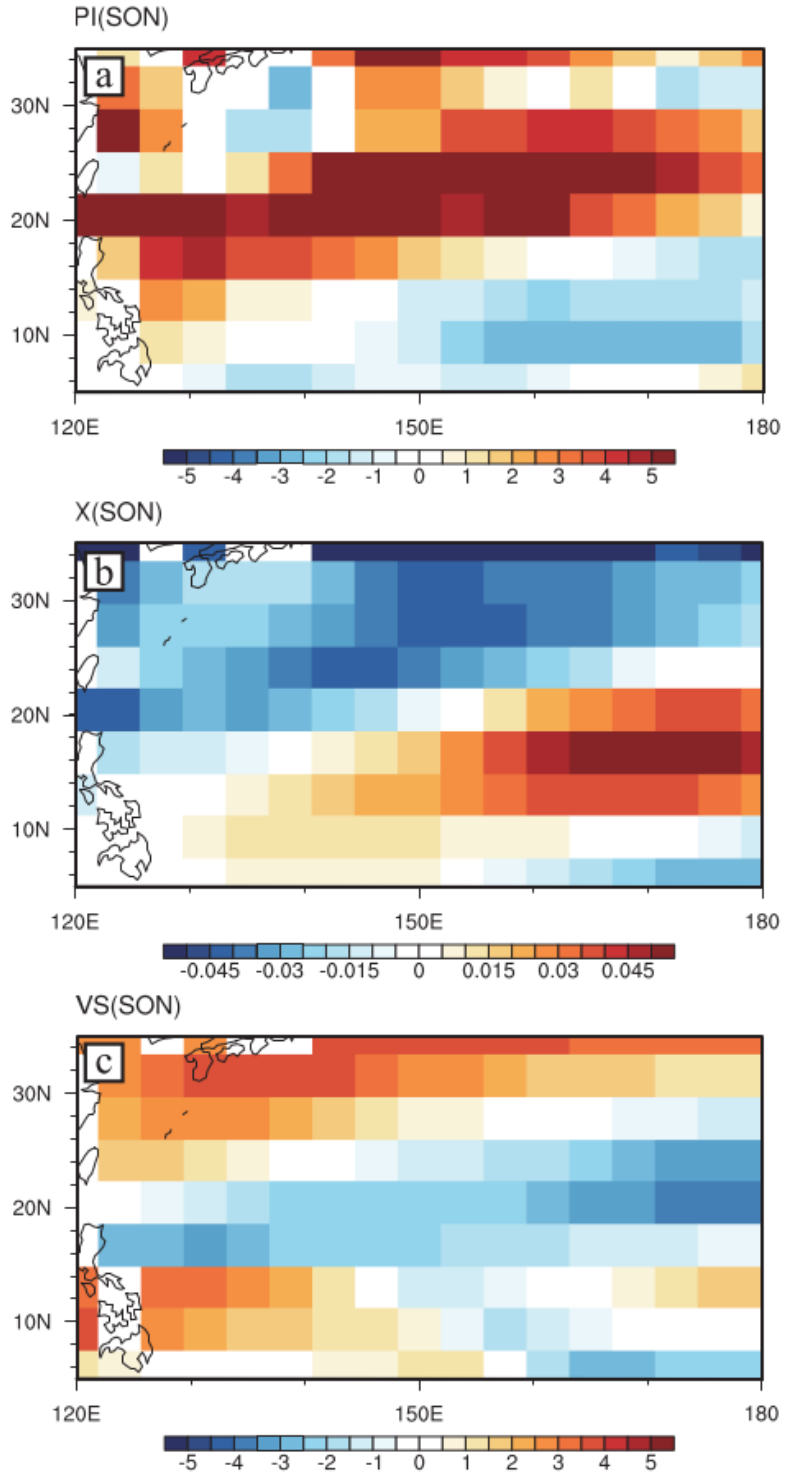

Figure S11. Trends (per 10 ka) of (a) potential intensity (units: m s^{-1}), (b) moist entropy deficit, and (c) vertical wind shear (units: m s^{-1}) from the mid-Holocene to the present (6–0 ka) in autumn in the TraCE-ORB experiment.